

Original Research

Rapamycin protects against neuronal death and improves neurological function with modulation of microglia after experimental intracerebral hemorrhage in rats

D. Li^{1,2}, F. Liu², T. Yang^{1,2}, T. Jin^{1,2}, H. Zhang^{1,2}, X. Luo², M. Wang^{1*}

¹ Department of Neurosurgery, First Affiliated Hospital of Xi'an Jiaotong University, Xi'an 710061, PR China

² Department of Neurosurgery, Ankang Central Hospital, Ankang 725000, PR china

Abstract: Intracerebral hemorrhage (ICH) results in a devastating brain disorder with high mortality and poor prognosis and effective therapeutic intervention for the disease remains a challenge at present. The present study investigated the neuroprotective effects of rapamycin on ICH-induced brain damage and the possible involvement of activated microglia. ICH was induced in rats by injection of type IV collagenase into striatum. Different dose of rapamycin was systemically administrated by intraperitoneal injection beginning at 1 h after ICH induction. Western blot analysis showed that ICH led to a long-lasting increase of phosphorylated mTOR and this hyperactivation of mTOR was reduced by systemic administration of rapamycin. Rapamycin treatment significantly improved the sensorimotor deficits induced by ICH, and attenuated ICH-induced brain edema formation as well as lesion volume. Nissl and Fluoro-Jade C staining demonstrated that administration with rapamycin remarkably decreased neuronal death surrounding the hematoma at 7 d after ICH insult. ELISA and real-time quantitative PCR demonstrated that rapamycin inhibited ICH-induced excessive expression of TNF- α and IL-1 β in ipsilateral hemisphere. Furthermore, activation of microglia induced by ICH was significantly suppressed by rapamycin administration. These data indicated that treatment of rapamycin following ICH decreased the brain injuries and neuronal death at the peri-hematoma striatum, and increased neurological function, which associated with reduced the levels of proinflammatory cytokines and activated microglia. The results provide novel insight into the neuroprotective therapeutic strategy of rapamycin for ICH insult, which possibly involving the regulation of microglial activation.

Key words: Intracerebral hemorrhage, rapamycin, mTOR, neuroprotection, neurological deficit, microglia.

Introduction

Intracerebral hemorrhage (ICH) is a subtype of stroke with high morbidity and mortality, which accounts for 8% to 15% of all strokes in Western populations and 20% to 30% in Asian and black populations (1, 2). Due to the mechanical destruction caused by blood accumulation, the acute cellular injury occurs immediately after ICH (3, 4). Furthermore, the toxic factors released from blood clot contribute to the inflammatory response of brain tissues, result in the formation of perihematomal edema, and the delayed or secondary neuronal death, which leads to severe neurological deficits (5-7).

The suppression of inflammatory cascades has been reported to reduce brain edema and neuronal damage, and improve neurological outcome in experimental ICH. Atorvastatin, a cholesterol-lowering drug, can play an anti-inflammatory role which reduces the perihematomal cell death after experimental ICH in rat (8, 9). Minocycline, a semisynthetic tetracycline, inhibits the microglial activation followed ICH and alleviates the degree of neuropathology (10, 11). Immuno-modulating agent cyclosporin A and tacrolimus have also been demonstrated to suppress the inflammatory response to experimental stroke insult and have neuroprotective effect (12, 13). These drugs improve neurological functions, reduce lesion volume and neuronal death in animals (14, 15). Hence, anti-inflammatory agents may be new therapeutic strategies for providing protection brain against ICH insult (16, 17).

Rapamycin (RAP), initially developed as an anti-fungal agent, was found to inhibit immune reactions and decrease cell proliferation (18). Its intracellular

target, mammalian target of rapamycin (mTOR), is an evolutionarily conserved serine/threonine kinase that plays important roles in the regulation of cell growth and metabolism by involving the anti-apoptotic signals, autophagy, transcription, translation, and cytoskeletal organization (19, 20). Dysfunction of phosphorylation of mTOR have been found in traumatic brain injury (21), Alzheimer's disease (22), tuberous sclerosis (23) and ischemic stroke (24), mTOR inhibitors have also been shown to improve the neurological behavioral in the animal model of the diseases (25, 26). These observations promote us to investigate the effects of rapamycin on ICH-induced brain injury in experimental model of rats.

In the present study, we examined the ICH-induced activation of mTOR signal in striatum and frontal cortex of suffering cerebral hemisphere. Then we further investigated whether rapamycin, when administered after ICH, can reduce brain edema and inflammation, and subsequently attenuate neuronal death and promote neurological recovery in a rat model of ICH.

Received April 22, 2016; Accepted September 23, 2016; Published September 30, 2016

* **Corresponding author:** Maode Wang, Department of Neurosurgery, 1st Affiliated Hospital, Xi'an Jiaotong University, Xi'an 710061, PR China. Email: wangmd33@163.com

Copyright: © 2016 by the C.M.B. Association. All rights reserved.

Materials and Methods

Rat ICH model

The rat ICH model was made by intrastriatal collagenase injection as previously reported (27), with some modifications. Briefly, adult male Sprague-Dawley rats (weighing 250 g to 300 g, purchased from the Experimental Animal Center of Xi'an Jiaotong University College of Medicine) were anesthetized using 10% chloral hydrate (3.5–4.0 ml/kg, *i.p.*) and placed prone onto a stereotaxic frame (Narishige, Tokyo, Japan). After the bregma was exposed, a borehole (1mm in diameter) was drilled through the skull for collagenase injection and then a microinjector needle was inserted. The following injecting coordinate was used: 1.1 mm posterior and 1.9 mm right lateral to bregma, and 3.4 mm ventral to the skull surface. For the ICH induction, 1 μ l of type IV collagenase (0.15 IU/ μ l, Sigma) was infused into the right striatum over a period of 5 min. The needle was allowed to stay *in situ* for another 10 min before it was slowly withdrawn. During operation, the temperature was monitored and maintained at $37 \pm 0.5^\circ\text{C}$ until the rat revived from anesthetization. Animals were recovered in room temperature with free access to food and water under a 12-hour light/dark cycle. All procedures were carried out in compliance with the guidelines of the Experimental Animal Center of Xi'an Jiaotong University Health Science Center. All experiments were performed in accordance with the National Institutes of Health Guide for the care and use of laboratory animals (NIH Publication No. 80-23, revised 1996). All efforts were made to minimize animals' suffering and to keep the numbers of animals used to a minimum.

Drug and experimental groups

Rapamycin was purchased from Sigma-aldrich (V900930). The dose of rapamycin used in the rat was ratiocinated by the adult human maintenance dose (2–4 mg/d). The drug powder was dissolved in dimethyl sulfoxide (DMSO; Sigma-aldrich; D2650). The doses of the drug in the experiment were set at 50, 150 and 450 μ g/kg weight, and administered in a volume not exceeding 1 ml/kg, intraperitoneal injection.

The rats were randomly divided into 6 groups. The first group did not receive any treatments and served as a normal control. The second group was sham operated. The third group was the ICH control. The rats of the fourth group received vehicle (DMSO) treatment. The fifth, sixth and seventh group were induced ICH and administered by 50, 150 and 450 μ g/kg of rapamycin, respectively. Group three to seven were induced ICH. The fourth to seventh group received vehicle or different dose of rapamycin intraperitoneal injection 1 h after ICH induction. Neurological deficits were evaluated at 2 h, 1 d, 3 d, 7 d and 14 d after ICH induction ($n=8$ for each group). To examine activation of mTOR, rats were euthanized at 1 d, 3 d, 7 d 14 d and 28 d after ICH, and Western blot was performed ($n=3$ for each time point). For water content assay, rats were euthanized at 1 d and 3 d after ICH ($n=6$ for each group). For TNF- α and IL-1 β expression assay, rats were euthanized at 2 h, 1 d and 7 d after ICH, and then ELISA and real-time PCR were performed ($n=6$ for each group). For H&E, Nissl, Fluoro-Jade C and Iba-1 immunohistochemical staining, rats

were sacrificed and fixed at 3 d and/or 7 d after ICH ($n=3$ for each group).

Western blot analysis

Rats were euthanized at 1 d, 3 d, 7d, 14 d and 28 d after ICH. The brains were removed, and the ipsilateral hemispheres were separated. The brain tissue was lysed by RIPA lysis buffer (Pierce, Rockford, IL, USA) with protease inhibitor cocktail (Roche, IN) on ice, and then subjected to homogenate using a homogenizer (PT2100, Polytron, Switzerland) followed the ultrasound treatment for 5 min with an ultrasonic homogenizer (Sonics). Samples were cleared by centrifugation at 12,000 g at 4°C for 10 min, and protein concentration in each sample was determined by BCA assay. Equal amounts of protein (50 μ g per lane) were separated by 10% SDS-polyacrylamide gels and transferred to PVDF membranes. After blocked in 10% nonfat dry milk for 1 h, the membranes were incubated overnight at 4°C with the following primary antibodies: rabbit anti-phospho-mTOR polyclonal (1:2000, Cell Signaling; 5536), rabbit anti-mTOR polyclonal (1:2000, Cell Signaling; 2983), mouse anti- β -Actin monoclonal (1:10000, Sigma-Aldrich; A5316). After rinsed in three times in TBST (20 mM Tris, 150 mM NaCl and 0.05% Tween 20), the membranes were probed with horse radish peroxidase (HRP)-conjugated anti-rabbit (1:100000, Sigma) or anti-mouse (1:100,000, Sigma) IgG for 1 h at room temperature. The immunoreactive bands were further visualized by enhanced chemiluminescence (ECL, Pierce, USA), and X-ray film (Fujifilm, Japan) exposure. The data were collected with a gel imaging system (SynGene, UK) and analyzed using ImageJ software (version 1.61, NIH). The housekeeping β -actin was used as the internal control to normalize levels of target proteins. The experiments were performed on three rats at each time point, and all experiments were repeated at least three times.

Neurological scoring

Neurological testing was performed for assessing sensorimotor deficits, as previously described with minor modification (28). The behavioral evaluation includes the following tests: postural signs, gait disturbances, limb placing, beam balance, symmetry of muscle tone and spontaneous activity. The sum of partial scores represented the total neurological score, and possible scores ranged from 42 to 0, which was maximum 42 and 0 indicating healthy animal. The neurological examination was performed in a blinded fashion and at least 8 animals were using in each experimental group.

Brain water content

Rats were decapitated under deep isoflurane anesthesia 1 d or 3 d after ICH induction. After sacrifice, the brains were removed and separated into right and left hemispheres. The cerebral hemispheres were immediately weighed to obtain the wet weight, then dried in an oven at 100°C for 24 h to gain the dry weight, as previously described (29). The percentage of brain water content was calculated using the following formula: $[(\text{wet weight} - \text{dry weight}) / \text{wet weight}] \times 100\%$.

Brain tissue fixation and frozen section

For histological staining, the rats were fixed by transcardial perfusion with 4% paraformaldehyde in PBS and postfixed overnight. After cytoprotection with 30% sucrose for about 2-3 days, brains were cut into coronal sections (20 μ m) using a freezing microtome (Leica, Germany) and the sections were mounted onto gelatinized slides and allowed to dry at room temperature. Brain sections containing hematoma and all of its surrounding lesion area (From bregma -0.2 mm to bregma -2.2 mm) were selected and divided into four groups (for each group, select one every three sections), for H&E, Nissl and Fluoro-Jade C and Iba-1 immunohistochemical staining, respectively.

Measurement of the ICH lesion volume

The ICH lesion volume was measured 3 d and 7 d following the ICH using H&E staining sections. The brain sections were stained with hematoxylin and eosin according a standard procedure. Pictures were taken using a microscope equipped with a 1.25X and 20 X objective and a digital camera (both from Olympus, Japan). ICH lesion area was defined by the presence of blood, tissue rarefaction and neuronal death (Fig 3B&C). The volume of ICH lesion was quantitated using a stereological method under Image-Pro Plus 5.0 software.

Fluoro-Jade C staining

Fluoro-Jade C staining was used to assess the dying neurons induced by ICH. Briefly, brain sections were incubated in 0.06% potassium permanganate gently shaking for 15 min and washed three times in distilled water, then sections were stained for 30 min by working solution of Fluoro-Jade C (Millipore; AG325) consisting of 10 ml 0.01% Fluoro-Jade C and 90 ml 0.1% acetic acid, followed by rinsed in distilled water for three times. After dried at room temperature in dark, the sections were mounted and observed using a using a BX51 fluorescent microscope equipped with a DP72 digital camera (both from Olympus, Japan). The number of Fluoro-Jade C positive neurons was counted immediately adjacent to hematomas and the sum of four fields from three sections was calculated for representing the number of Fluoro-Jade C positive cells per rat. All the counting was carried out in Image-Pro Plus 5.0 software (Olympus, Japan) and analyses were blindly evaluated.

ELISA Assay

In order to check the content of TNF- α and IL-1 β after rapamycin administration, the ELISA assay was carried out according to the manufacturer's instruction (R&D Systems, USA). In brief, Brain blocks 2 mm around the hematoma were collected at 2 h, 1 d and 7d after ICH. And then the protein was extracted with 1 ml PBS per 100 mg tissue by homogenization and centrifugation at 4 °C. For each ELISA analysis, 40 μ l of sample was used. The content of TNF- α and IL-1 β (ng/mg) was calculated using a standard curve method.

Real-time quantitative PCR

Expression of TNF- α and IL-1 β mRNA after rapamycin treatment was further examined using Real-time PCR. Brain block about 2 mm around the hematoma was isolated at 1 d and 7 d after ICH induction. The

total RNA was extracted using TRIzol Reagent (Invitrogen, USA) protocol according to the manufacturer's guidelines. RNA concentration was measured using absorbance at 260nm and the purity was determined using the ratio of absorbance at 260 and 280nm. And cDNA was synthesized using the ExScript™ RTase reagent kit (TaKaRa, Japan) with OligodT primers. Real-time quantitative PCR analyses were performed using SYBR Green I detection method in an ABI Prism 7000 Sequence detection system (Applied Biosystems, USA). The following primers were used: TNF- α -F: 5'- GGCCACCACGCTCTTCTGTC -3', TNF- α -R: 5'- GGGCTACGGGCTTGTCCTC -3', IL-1 β -F: 5'- CGATCGCGCAGGGGCTGGGCGG -3', IL-1 β -R: 5'-AGGAAGTACGGTACTGATGGA -3', GAPDH-F: 5'-GACAACCTTGGCATCGTGGA-3', GAPDH-R: 5'-ATGCAGGGATGATGTTCTGG-3'. After the PCR cycles, the PCR products were checked by running melting curve analysis. Amplification was performed in triplicate for each sample.

PCR data were analyzed at the termination of each assay using the Sequence Detector 1.0 software (Applied Biosystems, USA). The transcript level of each gene was calculated using the 2^{- $\Delta\Delta$ Ct} method as the following formula: $\Delta\Delta$ Ct = [Ct GI (unknown sample) - Ct GAPDH (unknown sample)] - [Ct GI (calibrator sample) - Ct GAPDH (calibrator sample)]. GAPDH was chosen as an internal control gene for normalizing transcript level of TNF- α and IL-1 β .

Immunohistochemical staining for Iba-1

Brain sections at 7 d after ICH were used to the immunohistochemical staining for Iba-1. In brief, after elimination endogenous peroxidase using 0.3% hydrogen peroxide for 10 min, the sections were permeabilized with 0.1% Triton X100 in PBS for 20 min, followed by block in 2% normal goat serum for 1 h. Then sections were incubated overnight with anti-Iba-1 mouse monoclonal antibody (1:400, Abcam, UK). After washing three times in PBS, the sections were incubated with biotin-conjugated goat anti-mouse IgG (1: 200, Vector laboratories, USA) for 2 h, followed incubation in avidin-biotin peroxidase complex (1:50, Vector laboratories, USA) for 1 h. Specific labeling was detected with 0.05% diaminobenzidine (DAB, Sigma-Aldrich) plus 0.005% H₂O₂. Iba-1 immunostaining positive cells were observed using a BX51 microscope equipped with a DP72 digital camera (both from Olympus, Japan). The number of Iba-1 positive microglia immediately adjacent to hematomas was counted and the sum of four fields from three sections was calculated for representing the number of positive cells per rat. All the counting was performed using a Image-Pro Plus 5.0 software and all analyses were blindly evaluated.

Statistics

All data are reported as mean \pm SD. Statistical analysis was performed using one-way ANOVA. Tukey's post-hoc analysis was used to determine the difference between treatments, and *p*-value < 0.05 was considered as statistical significance. All the statistical analysis was performed using SPSS for Windows (version 12.0; SPSS, USA).

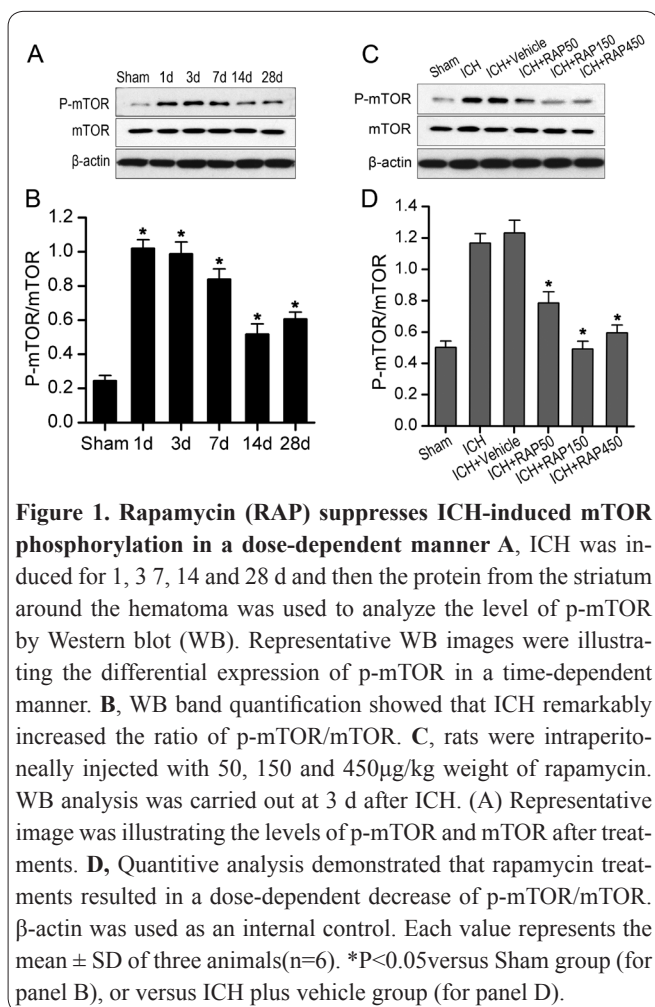


Figure 1. Rapamycin (RAP) suppresses ICH-induced mTOR phosphorylation in a dose-dependent manner **A**, ICH was induced for 1, 3, 7, 14 and 28 d and then the protein from the striatum around the hematoma was used to analyze the level of p-mTOR by Western blot (WB). Representative WB images were illustrating the differential expression of p-mTOR in a time-dependent manner. **B**, WB band quantification showed that ICH remarkably increased the ratio of p-mTOR/mTOR. **C**, rats were intraperitoneally injected with 50, 150 and 450 μg/kg weight of rapamycin. WB analysis was carried out at 3 d after ICH. **(A)** Representative image was illustrating the levels of p-mTOR and mTOR after treatments. **D**, Quantitative analysis demonstrated that rapamycin treatments resulted in a dose-dependent decrease of p-mTOR/mTOR. β-actin was used as an internal control. Each value represents the mean ± SD of three animals (n=6). *P<0.05 versus Sham group (for panel B), or versus ICH plus vehicle group (for panel D).

Results

Rapamycin inhibits mTOR phosphorylation induced by ICH insult in rats

We first observed the effects of ICH on the activation of mTOR signal in brain. Tissues from the ipsilateral striatum surrounding the hematoma were lysed at 1, 3, 7, 14 and 28 d after ICH, and Western blot analysis was used to illustrate the expression profile of phosphorylated mTOR (p-mTOR). The results showed that ICH caused a time-dependent increase of p-mTOR levels in the striatal tissue surrounding the hematoma from 1 d to 28 d after experimental ICH, while the expression of total mTOR was not significantly affected by ICH insult (Fig. 1A&B). These data suggest that ICH induced long-lasting activation of mTOR signaling.

In order to understand the effect of rapamycin on ICH-induced mTOR phosphorylation, rats suffering ICH were intraperitoneally injected by multiple dose of rapamycin (50, 150 and 450 μg/kg weight) beginning at 1 h after ICH, and Western blot analysis was carried out at 3 d after ICH. After rapamycin treatments, p-mTOR was significantly decreased in a dose-dependent manner, as compared to vehicle-treated group (Fig. 1C&D). Rapamycin at the dose of 150 μg/kg was shown the maximum action on inhibiting ICH-induced mTOR phosphorylation. No significant difference was observed in the expression of total mTOR between vehicle- and rapamycin-treated groups (Fig. 1).

Rapamycin alleviates the sensorimotor deficits after experimental ICH in rats

To demonstrate if rapamycin treatment has neuroprotective effects on ICH-induced injury in rats, neurological deficits were assessed at 2 h, 1 d, 3 d, 7 d and 14 d after ICH, with or without rapamycin injections. As shown in Fig. 2, There were no differences at any time in sham-operated group (P>0.05). However, neurological scores were remarkably increased following ICH for all time points (P<0.05) and there were significant differences among sham and ICH groups (P<0.05). Although there were no differences in the mean scores at 2 h after ICH among treated and untreated groups, a significant improvement in the mean scores was observed at 1 d, 3 d, 7 d and 14 d with rapamycin 150 and 450 μg/kg as compared to vehicle treated group (P<0.05), suggesting that rapamycin attenuated ICH-induced sensorimotor deficits in rats. Significant difference was not observed in the neurological performance between vehicle treated and 50 μg/kg rapamycin treated group (P>0.05).

Rapamycin reduces brain edema and lesion volume induced by experimental ICH in rats

To observe the effects of rapamycin on ICH-induced brain edema, the water contents in the ipsilateral hemisphere were measured at 1 d and 3 d after ICH (Fig. 3A). ICH resulted in significant elevation in water contents, as compared to sham treated group. There was no difference in water content between 50 μg/kg rapamycin and vehicle treated group, both at 1 d and 3 d after ICH (P>0.05). Treatment with 150 and 450 μg/kg rapamycin significantly decreased the water contents in ipsilateral hemisphere at both time points, as compared to vehicle treated groups (P<0.05), which indicates a significant improvement in ICH-induced brain edema.

We further assessed the role of rapamycin by determining the ICH lesion volume. Vehicle or 50, 150 and 450 μg/kg of rapamycin was administered beginning 1 h after ICH insult, for consecutive 3 d or 7 d. A series of H&E staining sections were used to measure the lesion volume (Fig. 3B&C). As shown in Fig. 3D, expect for 50 μg/kg of rapamycin group at 3 d, ICH lesion

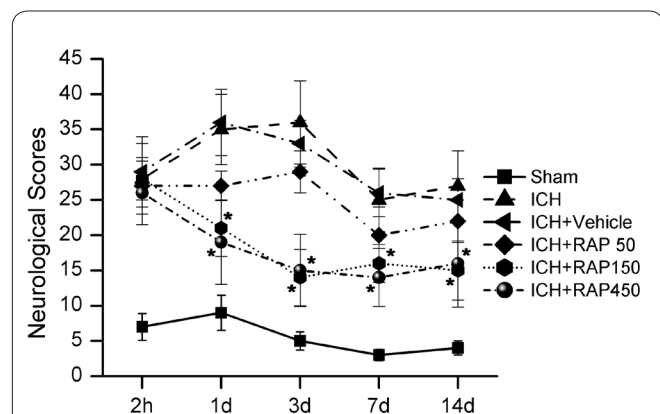


Figure 2. Effects of rapamycin (RAP) on Neurological function of rats suffered from ICH. The rats were induced ICH for 1 h following intraperitoneally injected with 50, 150 and 450 μg/kg weight of rapamycin. The neurological deficits were assessed at 2 h -14 d after ICH. The data showed that rapamycin significantly increased the neurological scores. Each value represents the mean ± SD of six animals (n=8) *P<0.05 versus ICH plus vehicle groups at each time point.

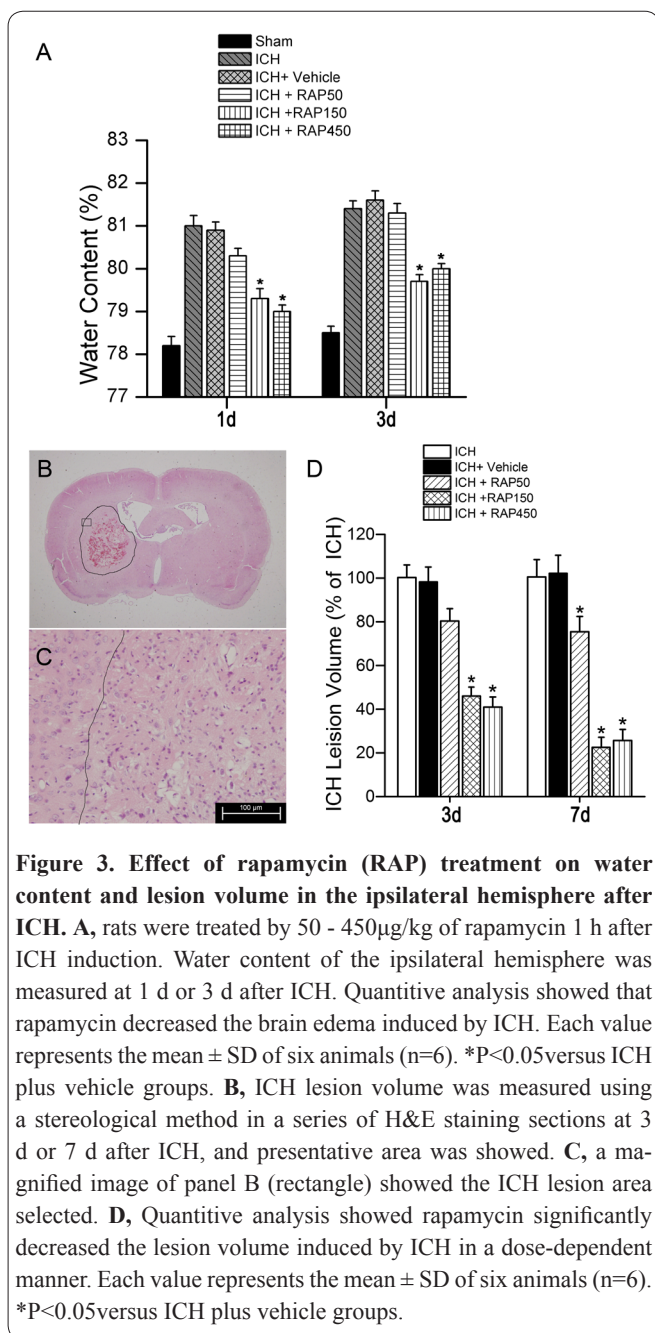


Figure 3. Effect of rapamycin (RAP) treatment on water content and lesion volume in the ipsilateral hemisphere after ICH. **A**, rats were treated by 50 - 450 μ g/kg of rapamycin 1 h after ICH induction. Water content of the ipsilateral hemisphere was measured at 1 d or 3 d after ICH. Quantitative analysis showed that rapamycin decreased the brain edema induced by ICH. Each value represents the mean \pm SD of six animals (n=6). *P<0.05 versus ICH plus vehicle groups. **B**, ICH lesion volume was measured using a stereological method in a series of H&E staining sections at 3 d or 7 d after ICH, and presentative area was showed. **C**, a magnified image of panel B (rectangle) showed the ICH lesion area selected. **D**, Quantitative analysis showed rapamycin significantly decreased the lesion volume induced by ICH in a dose-dependent manner. Each value represents the mean \pm SD of six animals (n=6). *P<0.05 versus ICH plus vehicle groups.

volume was significantly decreased in the rapamycin-treated groups at 3 d and 7 d, compared with the corresponding vehicle group. These results are consistent with the effect of rapamycin on neurological outcome in rats after ICH.

Rapamycin protects neurons against ICH injury in rats

To further determine the neuroprotective effect of rapamycin on ICH-induced brain injury, death of neurons surrounding the hematomas was observed at 7 d after ICH. Vehicle or 150 μ g/kg of rapamycin was administered beginning 1h after ICH insult and for 7 d. Nissl staining showed that vast of neurons were subjected to cell damage, which demonstrates cell shrinkage, karyopyknosis, even cell loss, as compared to Sham-operated group. However, rapamycin treatment significantly reduced the neuron injury (Fig. 4A-C). Furthermore, the dying neurons surrounding the hematomas were further observed using a Fluoro-Jade C staining (Fig. 4D-E). There were almost no Fluoro-Jade C positive cells in the sham-operated group. The number of dying neurons

was remarkably increased after ICH. Treatment using 150 μ g/kg of rapamycin significantly reduced the number of dying neurons induced by ICH (Fig. 4G), which suggests that rapamycin prevented neuron death following ICH insult in rats.

Rapamycin suppresses TNF- α and IL-1 β expression in brain after experimental ICH in rats

Expression of proinflammatory cytokines TNF- α and IL-1 β is reported to play an important role in inducing neuron death after stroke (30). We further examined the expression levels of TNF- α and IL-1 β in the ipsilateral striatum tissues upon rapamycin treatment after ICH. ELISA assay showed that ICH remarkably increased the levels of TNF- α and IL-1 β protein as compared to sham-operated group, and there were no significant differences among ICH and rapamycin treated groups at 2 h of ICH (P>0.05). Furthermore, these high level of the cytokines induced by ICH were significantly reduced in the rapamycin 150 and 450 groups at 1 d and 7 d (Fig. 5A&B, P<0.05), while the cytokine levels remained high upon 50 μ g/kg of rapamycin. Similarly, levels of TNF- α and IL-1 β mRNA were significantly increased after ICH insult, and treatment with rapamycin of a dose

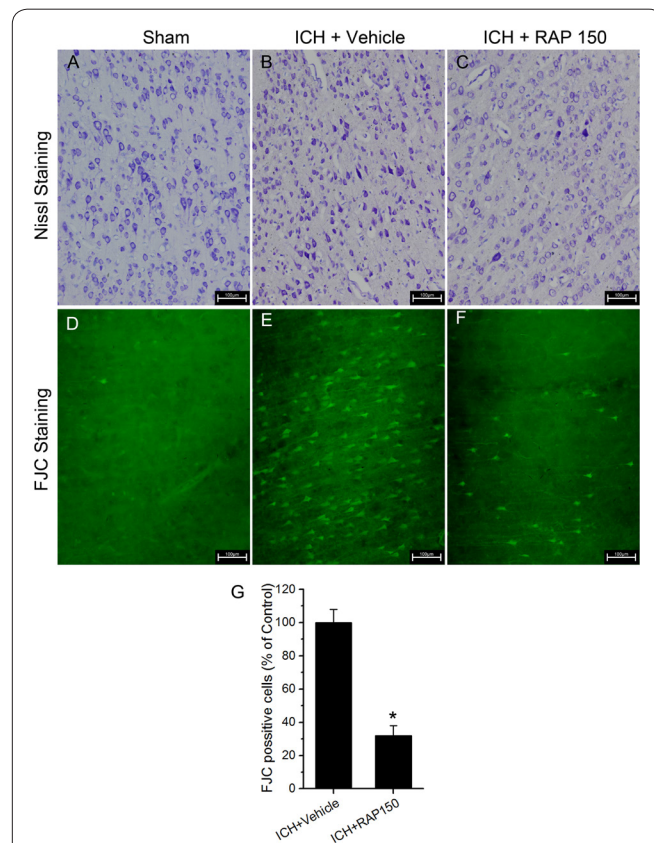
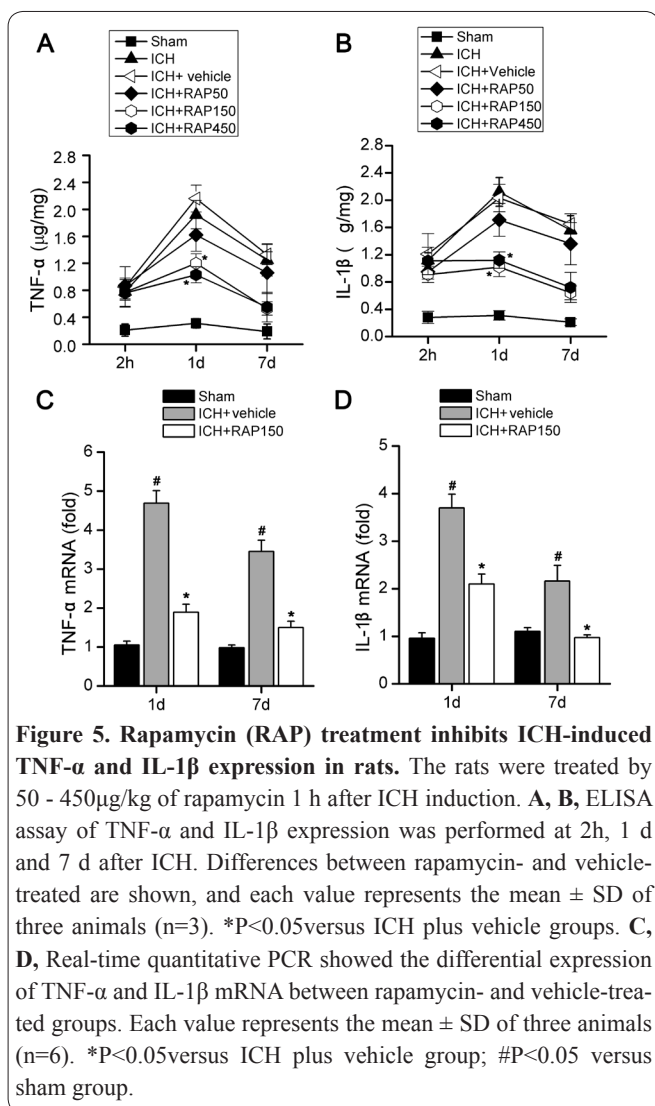


Figure 4. Rapamycin (RAP) treatment decreases the dying neurons induced by ICH. The rats with induced ICH were treated by 150 μ g/kg of rapamycin for 7 d, and Nissl and Fluoro-Jade C (FJC) staining were carried out at the paraffin sections. **A-C**, representative Nissl staining images showed the normal neurons (A), the injured neurons induced by ICH insult (B), and RAP treatment reduced the neuron injury (C). **D-F**, Representative images were illustrating the FJC positive neurons adjacent to hematomas in rats suffering from sham (D), ICH plus vehicle (E) and ICH plus RAP treatment (F). **G**, Quantitative comparison between RAP and vehicle-treated groups is demonstrated. Each value represents the mean \pm SD of three animals (n=5). *P<0.05 versus ICH plus vehicle group.



of 150 μ g/kg significantly decreased the high levels of both cytokines (Fig. 5C&D, $P>0.05$). These data indicate that rapamycin treatment suppressed ICH-induced expression of TNF- α and IL-1 β , which may result in death of neurons.

Rapamycin decreases activation of microglia after experimental ICH in rats

We next asked whether inhibition of ICH-induced microglia activation is involved in the neuroprotection of blocking mTOR signal by rapamycin. Activation of microglia after ICH was observed using Iba-1 (a marker of microglia) immunohistochemical staining method. Rapamycin (150 μ g/kg) or vehicle was administrated beginning 1h after ICH insult and for 7 d. Immunohistochemical staining showed that ICH insult resulted in significant activation of microglia, which are displayed by a morphological transformation that leads from the delicately ramified phenotype to cells with larger somata and coarser cytoplasmic processes (Fig. 6A&B). Moreover, the number of microglia after ICH was also increased, compared to that of the sham-operated group (Fig. 6D). However, rapamycin treatment significantly reduced the number of activated microglia, compared with the vehicle-treated group (Fig. 6C&D).

Discussion

The present study demonstrated a protective effect

of rapamycin on experimental ICH injury of brain. The major findings of this study are as follows: (1) ICH led to a long-lasting activation of mTOR signal in brain and this hyperactivation was reduced by systemic use of rapamycin; (2) Rapamycin reduced ICH-induced brain edema formation and lesion volume, protected neurons against damage and thereby attenuated neurological deficits after ICH insult; and (3) rapamycin suppressed ICH-induced activation of microglia and the excessive expression of TNF- α and IL-1 β , which may be one of the cellular and molecular mechanisms that neuroprotective effects of rapamycin after ICH in rats. These data indicate that rapamycin may be used as a new drug candidate in therapy of ICH insult.

ICH is a devastating brain disorder with high mortality and poor prognosis and effective therapeutic intervention for the disease remains a challenge at present (16, 31). Hemorrhage resulting from destroying of microvascular walls occurs preferentially in several brain regions including the striatum, the internal capsule and the thalamus (1, 2). Experimental rat models of ICH, based on intrastriatal injection of collagenase that disrupts basal lamina of blood vessels or autologous blood into the striatum (3), have been well developed, which greatly contributed to understanding of the cellular and molecular mechanisms in pathogenic events of ICH, and exploring potential therapeutic strategies as well (31-33). Compared to autologous blood, collagenase injection is more suitable for mimicking the disruption of central branches of cerebral arteries, which usually results in capsula interna haemorrhage in human (34). By utilizing striatal injection of collagenase to induce ICH in rats, and the present study observed the involvement of activation of mTOR signal in ICH injury of brain and explored the potential neuroprotective effect of rapamycin, an mTOR inhibitor.

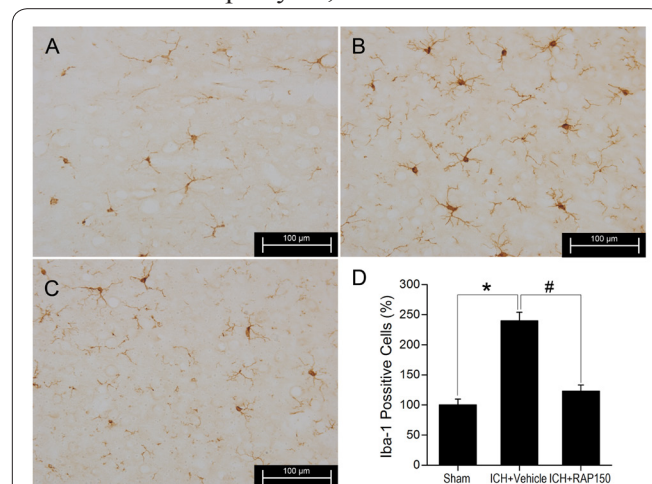


Figure 6. Rapamycin (RAP) treatment inhibits ICH-induced microglia activation in rats. The rats induced ICH were treated by 150 μ g/kg of rapamycin for 7 d, and the activation of microglia was showed using an Iba-1 (a marker for microglia) immunohistochemical staining method. **A-C**, Representative images are illustrating the FJC positive neurons adjacent to hematomas in rats suffering from sham-operation (A), ICH plus vehicle (B) and ICH plus RAP treatment (C). **D**, Quantitative analysis showed that rapamycin remarkably decreased the number of Iba-1 positive cells induced by ICH. Each value represents the mean \pm SD of three animals (n=6). *P<0.05 versus Sham group, #P<0.05 versus ICH plus RAP group.

mTOR is ubiquitous in various cell types throughout the body, which can influence a variety of physiological processes, including cell growth, proliferation, metabolism, protein synthesis and autophagy (19, 35, 36). mTOR also plays crucial roles in brain-specific mechanisms, such as synaptic plasticity, learning and memory, and brain development. However, abnormal mTOR signaling may promote the development of disease under pathophysiological conditions, such as diabetes, tumor and cardiovascular disease (36, 37). In addition, dysregulation of mTOR has also been implicated in a variety of neurological disorders, including astrocytoma, traumatic brain injuries, epilepsy, neurodevelopmental disorders and neurodegenerative diseases as well, in which hyperactivation of mTOR is involved in the cellular / molecular events of these diseases (19, 38-40). Furthermore, activation of mTOR has been reported in the development of the cerebrovascular diseases such as cerebral ischemia, ICH and subarachnoid hemorrhage (41-44). Consistently, our experiment showed a long-lasting activation of mTOR from 1 d to 28 d post ICH, accompanying with damage of brain tissue and neurological functions. Studies of other researchers and us suggested that activation of mTOR may be one of important factors in response to ICH insult. Due to the complexity of ICH-induced pathophysiological mechanisms, which may refer to the interaction of cellular events (reactive astrocytes and microglia) and release of molecules such as heme and iron, thrombin, matrix metalloproteinases and inflammatory cytokines (2, 7, 45, 46), further detail investigation need to be carried out for exploring the links among these cellular events and ICH-induced mTOR activation

Rapamycin, a specific inhibitor for mTOR, has been shown to provide neuroprotection after CNS disorders. For example, in an experimental model of Parkinson's disease, treatment with rapamycin reduced in dopaminergic neuronal death, increased the levels of anti-apoptotic protein Bcl-2 and induced autophagy and lysosomal biogenesis (47, 48). In animal model of Alzheimer's disease, rapamycin inhibited hyperactivation of mTOR, decreased phosphorylation of tau and formation of amyloid-beta, and contributed to improvement in cognitive deficits (22, 49). In experimental traumatic brain injury models, rapamycin was indicated to play neuroprotective roles, this mainly attributed to the reduction of microglia activation and induction of autophagy (26, 50). Moreover, rapamycin is also reported to improve the neurological outcome in experimental ICH (44) and focal cerebral ischemia in rats (24). Consistently, our study demonstrated that rapamycin, via inhibition of mTOR phosphorylation, significantly attenuated ICH-induced sensorimotor deficits. Furthermore, administration of the drug was shown the neuroprotective roles against ICH insult in reducing brain edema, lesion volume and neuronal death as well.

One of the key roles of mTOR is the regulation of immune and inflammatory responses (51, 52). During the development of ICH injury, with the destruction of blood-brain barrier and stimulation of released molecules in hematoma, circulatory and resided immune cells (microglia) are activated and subsequently mediated the immune responses in suffered brain, which resulting in acute brain damage and even persistent neuron

loss (3, 7, 51, 52). And immunosuppressive treatment after traumatic, ischemic or hemorrhagic brain damage has been reported to play a neuroprotective role (14, 51, 53). Minocycline, which inhibit activation of microglia, was shown to attenuate iron overload and brain injury after experimental ICH (10). Immune and inflammatory responses to ICH insult is also related to the release of proinflammatory cytokines, such as TNF- α and IL-1 β , which result in the death of neurons (54, 55). Rapamycin, an immunophilin ligand binding to mTOR, inhibiting the activation of mTOR, plays an immunosuppressive role in microglial response to brain and spinal cord injury (12, 51, 56). In the present experiments, we found rapamycin can reduce the TNF- α and IL-1 β expression and inhibit the activation of microglia, which may be one of the underlying mechanisms of neuroprotective effect of rapamycin against ICH insult. Moreover, reduction of TNF- α and IL-1 β expression may possibly due to the modulation of rapamycin on microglial activation after ICH, the detail cellular and molecular cascades remain unclear and need further investigation in an *in vitro* experimental system. In addition, other mechanisms, e.g. induction of autophagy, may contribute to the neuroprotection of rapamycin in our study, and further experiment should to be performed to clear the possibility, especially for the delayed or secondary neuronal loss after ICH insult.

In conclusion, the present study showed inhibition of rapamycin on the phosphorylation of mTOR in the experimental ICH model in rats, which decreased the brain damage and neuronal death, and attenuated neurological deficits. Furthermore, rapamycin inhibited the activation of microglia and reduced the expression levels of proinflammatory cytokines TNF- α and IL-1 β , which may be involved in the effect of the drug in protecting brain against ICH insult. These results may provide a novel insight into the neuroprotective therapeutic strategy of rapamycin for ICH, which possibly involving the regulation of microglial activation.

Acknowledgement

This study was supported by a grant from National Natural Science Foundation of China (No. 81371349).

References

1. Qureshi AI, Tuhim S, Broderick JP, Batjer HH, Hondo H, Hanley DF. Spontaneous intracerebral hemorrhage. *N Engl J Med* 2001; 344(19): 1450-60.
2. Qureshi AI, Mendelow AD, Hanley DF. Intracerebral haemorrhage. *Lancet* 2009; 373(9675): 1632-44.
3. Gong C, Hoff JT, Keep RF. Acute inflammatory reaction following experimental intracerebral hemorrhage in rat. *Brain Res* 2000; 871(1): 57-65.
4. Di Napoli M, Parry-Jones AR, Smith CJ, Hopkins SJ, Slevin M, Masotti L, *et al.* C-reactive protein predicts hematoma growth in intracerebral hemorrhage. *Stroke* 2014; 45(1): 59-65.
5. Hua Y, Nakamura T, Keep RF, Wu J, Schallert T, Hoff JT, *et al.* Long-term effects of experimental intracerebral hemorrhage: the role of iron. *J Neurosurg* 2006; 104(2): 305-12.
6. Perez de la Ossa N, Sobrino T, Silva Y, Blanco M, Millan M, Gomis M, *et al.* Iron-related brain damage in patients with intracerebral hemorrhage. *Stroke* 2010; 41(4): 810-3.
7. Power C, Henry S, Del Bigio MR, Larsen PH, Corbett D, Imai

- Y, *et al.* Intracerebral hemorrhage induces macrophage activation and matrix metalloproteinases. *Ann Neurol* 2003; 53(6): 731-42.
8. Jung KH, Chu K, Jeong SW, Han SY, Lee ST, Kim JY, *et al.* HMG-CoA reductase inhibitor, atorvastatin, promotes sensorimotor recovery, suppressing acute inflammatory reaction after experimental intracerebral hemorrhage. *Stroke* 2004; 35(7): 1744-9.
 9. Karki K, Knight RA, Han Y, Yang D, Zhang J, Ledbetter KA, *et al.* Simvastatin and atorvastatin improve neurological outcome after experimental intracerebral hemorrhage. *Stroke* 2009; 40(10): 3384-9.
 10. Zhao F, Hua Y, He Y, Keep RF, Xi G. Minocycline-induced attenuation of iron overload and brain injury after experimental intracerebral hemorrhage. *Stroke* 2011; 42(12): 3587-93.
 11. Xue M, Mikliaeva EI, Casha S, Zygun D, Demchuk A, Yong VW. Improving outcomes of neuroprotection by minocycline: guides from cell culture and intracerebral hemorrhage in mice. *Am J Pathol* 2010; 176(3): 1193-202.
 12. Gupta YK, Chauhan A. Potential of immunosuppressive agents in cerebral ischaemia. *Indian J Med Res* 2011; 133: 15-26.
 13. Shiga Y, Onodera H, Matsuo Y, Kogure K. Cyclosporin A protects against ischemia-reperfusion injury in the brain. *Brain Res* 1992; 595(1): 145-8.
 14. Nito C, Ueda M, Inaba T, Katsura K, Katayama Y. FK506 ameliorates oxidative damage and protects rat brain following transient focal cerebral ischemia. *Neurol Res* 2011; 33(8): 881-9.
 15. Furuichi Y, Noto T, Li JY, Oku T, Ishiye M, Moriguchi A, *et al.* Multiple modes of action of tacrolimus (FK506) for neuroprotective action on ischemic damage after transient focal cerebral ischemia in rats. *Brain Res* 2004; 1014(1-2): 120-30.
 16. Rincon F, Mayer SA. Intracerebral hemorrhage: clinical overview and pathophysiologic concepts. *Transl Stroke Res* 2012; 3(Suppl 1): 10-24.
 17. Mattson MP, Culmsee C, Yu ZF. Apoptotic and antiapoptotic mechanisms in stroke. *Cell Tissue Res* 2000; 301(1): 173-87.
 18. Kamada Y, Sekito T, Ohsumi Y. Autophagy in yeast: a TOR-mediated response to nutrient starvation. *Curr Top Microbiol Immunol* 2004; 279: 73-84.
 19. Wong M. Mammalian target of rapamycin (mTOR) pathways in neurological diseases. *Biomed J* 2013; 36(2): 40-50.
 20. Lei C, Wu B, Cao T, Zhang S, Liu M. Activation of the high-mobility group box 1 protein-receptor for advanced glycation end-products signaling pathway in rats during neurogenesis after intracerebral hemorrhage. *Stroke* 2015; 46(2): 500-6.
 21. Chen S, Atkins CM, Liu CL, Alonso OF, Dietrich WD, Hu BR. Alterations in mammalian target of rapamycin signaling pathways after traumatic brain injury. *J Cereb Blood Flow Metab* 2007; 27(5): 939-49.
 22. Caccamo A, Majumder S, Richardson A, Strong R, Oddo S. Molecular interplay between mammalian target of rapamycin (mTOR), amyloid-beta, and Tau: effects on cognitive impairments. *J Biol Chem* 2010; 285(17): 13107-20.
 23. Ehninger D, Han S, Shilyansky C, Zhou Y, Li W, Kwiatkowski DJ, *et al.* Reversal of learning deficits in a Tsc2^{+/-} mouse model of tuberous sclerosis. *Nat Med* 2008; 14(8): 843-8.
 24. Chauhan A, Sharma U, Jagannathan NR, Reeta KH, Gupta YK. Rapamycin protects against middle cerebral artery occlusion induced focal cerebral ischemia in rats. *Behav Brain Res* 2011; 225(2): 603-9.
 25. Guo D, Zeng L, Brody DL, Wong M. Rapamycin attenuates the development of posttraumatic epilepsy in a mouse model of traumatic brain injury. *PLoS One* 2013; 8(5): e64078.
 26. Erlich S, Alexandrovich A, Shohami E, Pinkas-Kramarski R. Rapamycin is a neuroprotective treatment for traumatic brain injury. *Neurobiol Dis* 2007; 26(1): 86-93.
 27. Wu H, Wu T, Xu X, Wang J. Iron toxicity in mice with collagenase-induced intracerebral hemorrhage. *J Cereb Blood Flow Metab* 2011; 31(5): 1243-50.
 28. Reglodi D, Tamas A, Lengvari I. Examination of sensorimotor performance following middle cerebral artery occlusion in rats. *Brain Res Bull* 2003; 59(6): 459-66.
 29. Tsubokawa T, Solaroglu I, Yatsushige H, Cahill J, Yata K, Zhang JH. Cathepsin and calpain inhibitor E64d attenuates matrix metalloproteinase-9 activity after focal cerebral ischemia in rats. *Stroke* 2006; 37(7): 1888-94.
 30. Liesz A, Middelhoff M, Zhou W, Karcher S, Illanes S, Veltkamp R. Comparison of humoral neuroinflammation and adhesion molecule expression in two models of experimental intracerebral hemorrhage. *Exp Transl Stroke Med* 2011; 3(1): 11.
 31. Xi G, Keep RF, Hoff JT. Mechanisms of brain injury after intracerebral haemorrhage. *Lancet Neurol* 2006; 5(1): 53-63.
 32. Katsuki H. Exploring neuroprotective drug therapies for intracerebral hemorrhage. *J Pharmacol Sci* 2010; 114(4): 366-78.
 33. Auriat AM, Silasi G, Wei Z, Paquette R, Paterson P, Nichol H, *et al.* Ferric iron chelation lowers brain iron levels after intracerebral hemorrhage in rats but does not improve outcome. *Exp Neurol* 2012; 234(1): 136-43.
 34. Mracsko E, Javidi E, Na SY, Kahn A, Liesz A, Veltkamp R. Leukocyte invasion of the brain after experimental intracerebral hemorrhage in mice. *Stroke* 2014; 45(7): 2107-14.
 35. Pastor MD, Garcia-Yebenes I, Fradejas N, Perez-Ortiz JM, Mora-Lee S, Tranque P, *et al.* mTOR/S6 kinase pathway contributes to astrocyte survival during ischemia. *J Biol Chem* 2009; 284(33): 22067-78.
 36. Zoncu R, Efeyan A, Sabatini DM. mTOR: from growth signal integration to cancer, diabetes and ageing. *Nat Rev Mol Cell Biol* 2011; 12(1): 21-35.
 37. Dazert E, Hall MN. mTOR signaling in disease. *Curr Opin Cell Biol* 2011; 23(6): 744-55.
 38. Li J, Kim SG, Blenis J. Rapamycin: one drug, many effects. *Cell Metab* 2014; 19(3): 373-9.
 39. Bove J, Martinez-Vicente M, Vila M. Fighting neurodegeneration with rapamycin: mechanistic insights. *Nat Rev Neurosci* 2011; 12(8): 437-52.
 40. Park J, Zhang J, Qiu J, Zhu X, Degterev A, Lo EH, *et al.* Combination therapy targeting Akt and mammalian target of rapamycin improves functional outcome after controlled cortical impact in mice. *J Cereb Blood Flow Metab* 2012; 32(2): 330-40.
 41. Lu DY, Liou HC, Tang CH, Fu WM. Hypoxia-induced iNOS expression in microglia is regulated by the PI3-kinase/Akt/mTOR signaling pathway and activation of hypoxia inducible factor-1 α . *Biochem Pharmacol* 2006; 72(8): 992-1000.
 42. Jing CH, Wang L, Liu PP, Wu C, Ruan D, Chen G. Autophagy activation is associated with neuroprotection against apoptosis via a mitochondrial pathway in a rat model of subarachnoid hemorrhage. *Neuroscience* 2012; 213: 144-53.
 43. Chen CW, Chen TY, Tsai KL, Lin CL, Yokoyama KK, Lee WS, *et al.* Inhibition of autophagy as a therapeutic strategy of iron-induced brain injury after hemorrhage. *Autophagy* 2012; 8(10): 1510-20.
 44. Lu Q, Gao L, Huang L, Ruan L, Yang J, Huang W, *et al.* Inhibition of mammalian target of rapamycin improves neurobehavioral deficit and modulates immune response after intracerebral hemorrhage in rat. *J Neuroinflammation* 2014; 11: 44.
 45. Nakamura T, Keep RF, Hua Y, Schallert T, Hoff JT, Xi G. Dexamethasone-induced attenuation of brain edema and neurological deficits in a rat model of intracerebral hemorrhage. *J Neurosurg* 2004; 100(4): 672-8.
 46. Levy YS, Streifler JY, Panet H, Melamed E, Offen D. Hemin-

induced apoptosis in PC12 and neuroblastoma cells: implications for local neuronal death associated with intracerebral hemorrhage. *Neurotox Res* 2002; 4(7-8): 609-16.

47. Malagelada C, Jin ZH, Jackson-Lewis V, Przedborski S, Greene LA. Rapamycin protects against neuron death in in vitro and in vivo models of Parkinson's disease. *J Neurosci* 2010; 30(3): 1166-75.

48. Shen X, Ma L, Dong W, Wu Q, Gao Y, Luo C, *et al.* Autophagy regulates intracerebral hemorrhage induced neural damage via apoptosis and NF-kappaB pathway. *Neurochem Int* 2016; 96: 100-12.

49. Siman R, Cocca R, Dong Y. The mTOR Inhibitor Rapamycin Mitigates Perforant Pathway Neurodegeneration and Synapse Loss in a Mouse Model of Early-Stage Alzheimer-Type Tauopathy. *PLoS One* 2015; 10(11): e0142340.

50. Urbanek T, Kuczmik W, Basta-Kaim A, Gabryel B. Rapamycin induces protective autophagy in vascular endothelial cells exposed to oxygen-glucose deprivation. *Brain Res* 2014; 1553: 1-11.

51. Hailer NP. Immunosuppression after traumatic or ischemic CNS damage: it is neuroprotective and illuminates the role of microglial

cells. *Prog Neurobiol* 2008; 84(3): 211-33.

52. Phillis JW, Diaz FG, O'Regan MH, Pilitsis JG. Effects of immunosuppressants, calcineurin inhibition, and blockade of endoplasmic reticulum calcium channels on free fatty acid efflux from the ischemic/reperfused rat cerebral cortex. *Brain Res* 2002; 957(1): 12-24.

53. Sharkey J, Butcher SP. Immunophilins mediate the neuroprotective effects of FK506 in focal cerebral ischaemia. *Nature* 1994; 371(6495): 336-9.

54. Ewen T, Qiuting L, Chaogang T, Tao T, Jun W, Liming T, *et al.* Neuroprotective effect of atorvastatin involves suppression of TNF-alpha and upregulation of IL-10 in a rat model of intracerebral hemorrhage. *Cell Biochem Biophys* 2013; 66(2): 337-46.

55. Lu A, Tang Y, Ran R, Ardizzone TL, Wagner KR, Sharp FR. Brain genomics of intracerebral hemorrhage. *J Cereb Blood Flow Metab* 2006; 26(2): 230-52.

56. Song Q, Xie D, Pan S, Xu W. Rapamycin protects neurons from brain contusion-induced inflammatory reaction via modulation of microglial activation. *Mol Med Rep* 2015; 12(5): 7203-10.